VOLUME 117, NUMBER 43
NOVEMBER 1, 1995

JOURNAL OF THE AMERICAN CHEMICAL SOCIETY

Escherichia coli Imidazoleglycerol Phosphate Dehydratase: Spectroscopic Characterization of the Enzymic Product and the Steric Course of the Reaction

Aulma R. Parker, Jeffrey A. Moore, John M. Schwab,* and V. Jo Davisson*

Contribution from the Department of Medicinal Chemistry and Pharmacognosy, 1333 Robert E. Heine Pharmacy Building, Purdue University, West Lafayette, Indiana 47907-3013

Received May 11, 1995[⊗]

Abstract: Recombinant strains of *Escherichia coli* have been developed for the high-level production of imidazoleglycerol phosphate dehydratase (IGPD) and imidazoleacetol phosphate aminotransferase (IAP aminotransferase). These protein sources facilitated the determination of the IGPD reaction stereochemistry and enabled the development of a continuous spectrophotometric enzyme assay for the IGPD reaction. D-*erythro*-IGP and D-*erythro*-[3-^{2}H]IGP were generated using a chemoenzymatic approach. D-(−)-[3-^{2}H]Ribose-5-phosphate was prepared synthetically, starting from diacetone-D-glucose, and converted enzymatically to D-*erythro*-[3-^{2}H]IGP. In separate reactions, D-*erythro*-IGP and D-*erythro*-[3-^{2}H]IGP were converted to IAP using *E. coli* IGPD. The resulting IAP was transformed directly to histidinol using the coupled activities of *E. coli* IAP aminotransferase and histidinol phosphate phosphatase. The enzymatically generated histidinol samples were analyzed by ^{1}H and ^{2}H NMR and compared to a synthetically prepared sample of (2*S**,3*S**)-[3-^{2}H]histidinol. This analysis demonstrated that the *E. coli* IGPD reaction proceeds with inversion of configuration at C-3, and the proton added to C-3 of IAP during the course of the dehydration is derived from the solvent. The observed stereochemical outcome is consistent with the idea that if the IGPD reaction proceeds through an enol intermediate, then tautomerization of the enol to IAP must be enzyme-mediated. The product of the IGPD reaction, IAP, has been characterized by NMR spectroscopy in aqueous solution. IAP undergoes rapid exchange of the C-3 protons with the bulk medium and exists as a mixture of the ketone and its hydrate (a geminal diol). Additional solution chemistry of IAP was observed using UV−vis and EPR spectroscopy and is consistent with the idea that IAP coordinates to Mn^{2+} in a bi- or tridentate fashion in aqueous solutions.

Histidine was first isolated nearly a century ago, and its structure was elucidated in the early 1900s.[1] Although the genetics and metabolic regulation of histidine biosynthesis are well characterized,[2−4] relatively little is known about the histidine biosynthetic enzymes. Clearly, this is not due to a lack of interest in histidine biosynthesis. Since histidine is an

[⊗] Abstract published in *Advance ACS Abstracts*, October 1, 1995.

(1) Greenstein, J. P.; Winitz, M. *Chemistry of the Amino Acids*; John Wiley and Sons: New York, 1961.

(2) Artz, S. W.; Holzschu, D. In *Amino Acids: Biosynthesis and Genetic Regulation*; Herrmann, K. M., Somerville, R. L., Eds.; Addison-Wesley Publishing Co.: Reading, MA, 1983; pp 379−404.

(3) Winkler, M. E. In *Escherichia coli and Salmonella typhimurium*; Neidhardt, E. C., Ingraham, J.L., Low, K. B., Magasanik, B., Schaechler, M., Umbarger, H. E., Eds.; American Society Microbiology: Washington, DC, 1987; Vol. 1, pp 395−411.

(4) Blasi, F.; Bruni, C. B. *Curr. Top. Cell. Regul.* **1981**, *19*, 1−45.

(5) (a) Mori, I.; Pfister-Fonné, R.; Matsunaga, S.-i.; Tada, S.; Kimura, Y.; Iwasaki, G.; Mano, J.-i.; Hatano, M.; Nakano, T.; Koizumi, S.-i.; Scheidegger, A.; Hayakawa, K.; Ohta, D. *Plant Physiol.* **1995**, *107*, 719−723. (b) Mori, I.; Iwasaki, G.; Kimura, Y.; Matsunaga, S.-I.; Ogawa, A.; Nakano, T.; Buser, H.-P.; Hatano, M.; Tada, S.; Hayakawa, K. *J. Am. Chem. Soc.* **1995**, *117*, 4411−4412.

0002-7863/95/1517-10605$09.00/0

Scheme 1

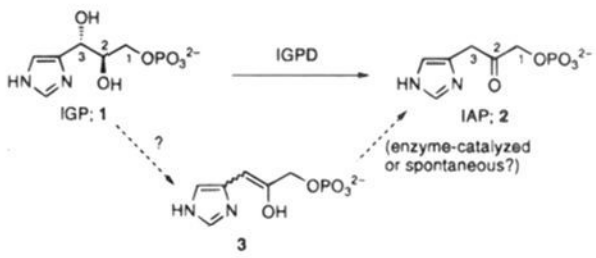

essential dietary nutrient for animals but is made *de novo* by microorganisms and plants, the histidine biosynthesis pathwayis a legitimate target for agrichemical discovery.[5] However, both the enzymes and many of the structurally complex pathway intermediates have been difficult to obtain, and so it is only recently that the mechanistically intriguing reactions in this pathway have become accessible for detailed study.

Imidazoleglycerol phosphate dehydratase (IGPD) catalyzes the net dehydration of imidazoleglycerol phosphate (IGP) to imidazoleacetol phosphate (IAP), a late intermediate in the histidine pathway. This reaction is unusual in that the vast majority of enzyme-catalyzed dehydrations are straightforward β-eliminations, in which the hydrogen that is lost is relatively acidic by virtue of its being adjacent to a carbonyl or imine functional group.[6] By contrast, the C-2 hydrogen of IGP is quite nonacidic, and so the mechanism by which it is removed *en route* to IAP is not obvious. As presented in the Discussion, a number of mechanisms for IGPD can be envisioned. We now report the first part of an effort to thoroughly characterize IGPD and the mechanism by which it converts IGP to IAP. (A preliminary account of the stereochemical analysis has been published.[7]) A chemoenzymatic preparation of the substrates and products for IGPD has been developed that allows for incorporation of stable isotopes into IGP. Efficiently overproducing strains of *Escherichia coli* have been established for the isolation of IGPD−histidinol phosphate (HP) phosphatase and IAP aminotransferase. Routine analysis of IGP turnover has been performed with a new, continuous, spectrophotometric assay that involves coupling to IAP aminotransferase. These methods have proven pivotal for a stereochemical analysis of the IGPD reaction and have led to the characterization of some unusual solution chemistry for IAP.

Results

Design of the Stereochemical Assay System. Two of the mechanisms that were considered for IGPD would entail direct transfer of the C-2 hydrogen of IGP to C-3 of IAP. The remaining mechanisms predict that the Δ^2-enol **3** is an intermediate *en route* to IAP. If this were so, then tautomerization of the enol to the keto form could be either enzyme-catalyzed or spontaneous (Scheme 1). Since any stereoselectivity in the IGPD reaction would be inconsistent with spontaneous, nonenzymatic ketonization of an achiral enol, the stereochemical course of the IGPD reaction was determined.

As shown below, the C-3 protons of IAP were expected to exchange readily in aqueous solution. This situation potentially complicates a stereochemical analysis of [3-^{2}H]IAP and prompted the design of a coupled reaction (Scheme 2) that converts IAP directly to HP by IAP aminotransferase (the *hisC* gene product). Since *hisB* is a bifunctional gene that encodes HP phosphatase in addition to IGPD, the ultimate product of this coupled system would be histidinol. As described below, the diastereotopic C-3 protons (deuterons) of histidinol are distinguishable by NMR spectroscopy.

Scheme 2

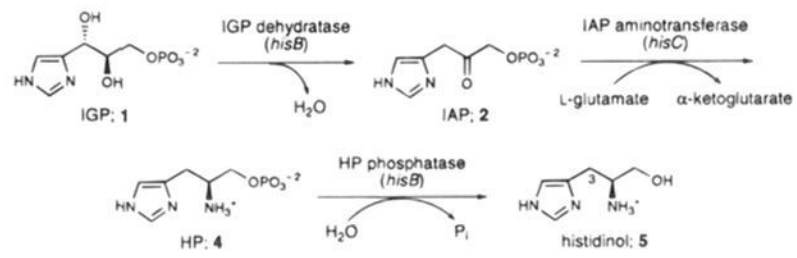

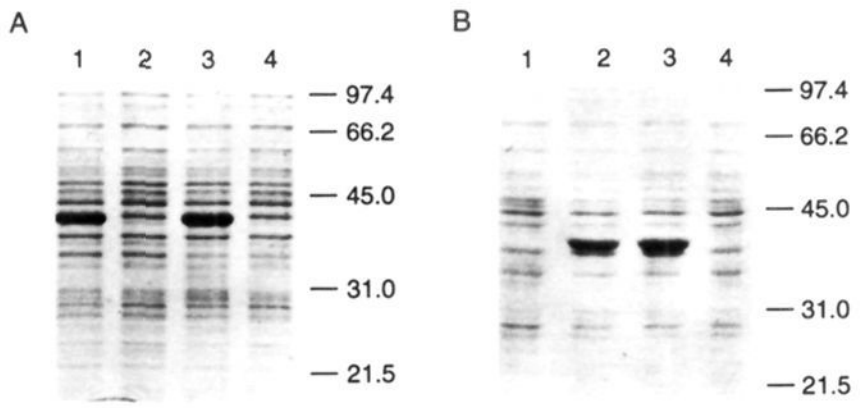

Figure 1. Coomassie-stained SDS−PAGE of IGPD and IAP aminotransferase: (A) production of *E. coli* IGPD in *E. coli* FB1 (lane 1, p*hisB-tac*, + IPTG, 2 h; lane 2, p*hisB-tac*, no IPTG, 2 h; lane 3, p*hisB-tac*, + IPTG, 6 h; lane 4, p*hisB-tac*, no IPTG, 6 h); (B) production of *E. coli* IAP aminotransferase in *E. coli* FB1) lane 1, p*hisC-tac*, no IPTG, 2 h; lane 2, p*hisC-tac*, + IPTG, 2 h; lane 3, p*hisC-tac*, + IPTG, 6 h; lane 4, p*hisC-tac*, no IPTG, 6 h. The predicted molecular weights of HisB and HisC are 40 283 and 39 319, respectively.

Cloning and Expression of *E. coli hisB* and *hisC*. To study IGPD reaction stereochemistry, dependable sources of the *hisB* and *hisC* gene products were required. Accordingly, *hisB* was cloned by the polymerase chain reaction (PCR) from plasmid pVG-2, which bears the genes associated with the late portion of the histidine biosynthesis pathway, and inserted into the *E. coli* expression vector pJF119EH.[8] The resulting construct p*hisB-tac* was transformed into the histidine operon mutant *E. coli* FB1, providing *E. coli* FB1-*hisB*. IGPD activity[9] was detected at 12 U/mg in the supernatant of *E. coli* FB1-*hisB* that had been disrupted by sonication or passage through a French pressure cell. Densitometric scans of SDS−polyacrylamide gels revealed that ca. 50% of the total cytosolic protein from this strain is HisB (Figure 1). While crude extracts were utilized for the studies described in this paper, approximately 100 mg of 90%-homogeneous protein can be obtained from 6 g of *E. coli* FB1-*hisB*, a quantity of cells that is obtained routinely from 1 L of culture.

The *hisC* gene was cloned in the same manner as was *hisB*, leading to *E. coli* FB1-*hisC*. IAP aminotransferase activity[9] was detected at 4 U/mg in the cell lysate supernatant from this strain, and ca. 40% of the total cytosolic protein from this strain was found to be HisC (Figure 1). Approximately 150−200 mg of purified IAP aminotransferase can be obtained from 6−8 g of *E. coli* FB1-*hisC*. As with HisB, crude HisC preparations were utilized for the stereochemical studies described in this paper.

In addition to being used for the semipreparative scale production of histidinol, the system shown in Scheme 2 was adapted for use in a continuous, coupled, spectrophotometric assay of IGPD activity (Scheme 3). In this assay, α-ketoglutarate is recycled to L-glutamate by the action of glutamate dehydrogenase in the presence of excess ammonium ion and NADH. The loss of absorbance at 340 nm (the λ_{max} for NADH) reflects the production of IAP from IGP. For the coupled assay,

(6) Gerlt, J. A.; Gassman, P. G. *J. Am. Chem. Soc.* **1992**, *114*, 5928−5934.

(7) Moore, J. A.; Parker, A. R.; Davisson, V. J.; Schwab, J. M. *J. Am. Chem. Soc.* **1993**, *115*, 3338−3339.

(8) Fürste, J. P.; Pansegrau, W.; Frank, R.; Blocker, H.; Scholz, P.; Bagdasarian, M.; Lanka, E. *Gene* **1986**, *48*, 119−131.

(9) Martin, R. G.; Berberich, M. A.; Ames, B. N.; Davis, W. W.; Goldberger, R. F.; Yourno, J. D. *Methods Enzymol.* **1971**, *17B*, 3−44.

Scheme 3

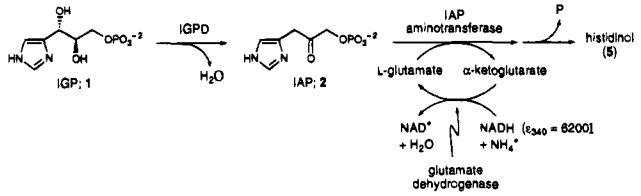

Scheme 4

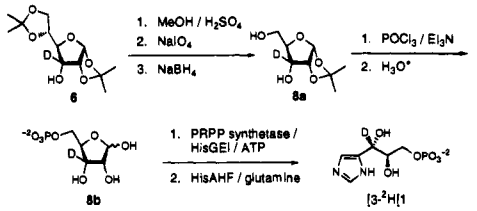

IAP aminotransferase of at least 95% homogeneity was utilized, Under these conditions, the assay is linear for the first 20 min, The initial lag time for the coupled IGPD assay is negligible (less than 15 s), when appropriate amounts of both coupling enzymes are utilized to ensure that the IGPD-catalyzed reaction is rate-limiting. (A similar version of this assay was reported during the preparation of this paper.[10]) (^{1}H and ^{13}C NMR spectra of IAP in H_2O and D_2O are included in the supporting information.)

Chemoenzymatic Synthesis of [3-^{2}H]IGP. The synthesis of [3-^{2}H]IGP (Scheme 4) was effected in two phases, Commercial diacetone-D-glucose (**6**) was transformed in 18% overall yield to [3-^{2}H]ribose-5-phosphate (**8b**), which was subsequently converted to N^1-[(5″-phospho-β-D-ribosyl)formimino]-5-aminoimidazole-4-carboxamide ribonucleotide (5′-ProFAR) by PRPP synthetase along with three enzymes from the *E. coli* histidine biosynthetic pathway via methods described previously.[11] Finally, HisA (5′-ProFAR isomerase) and HisH/F (IGP synthase)[12] were used to complete the synthesis of [3-^{2}H]IGP. The overall yield of [3-^{2}H]IGP from [3-^{2}H]ribose-5-phosphate was 30%.

Enzyme-Catalyzed Conversion of IGP to Histidinol. [3-^{2}H]IGP was converted to [3-^{2}H]histidinol by the coupled enzyme system shown in Scheme 2. The same system (albeit in D_2O- rather than H_2O-based buffer) was used for the conversion of unlabeled IGP to [2,3-^{2}H]histidinol, (Deuterium is exchanged in at C-2 by the pyridoxal phosphate-dependent aminotransferase.) [2,3,3-^{2}H]Histidinol was made analogously, but by using only one-fourth the optimal amount of HisB protein and only 1−2% of the usual HisC protein and L-glutamate levels, Under these conditions, the C-3 protons of IAP underwent complete exchange prior to transamination,

Synthesis of (2*S,3*S**)-[3-^{2}H]Histidinol.** In order to make unequivocal assignments of the NMR signals corresponding to protons (or deuterons) at C-3 of histidinol, a sample of (2*S**,3*S**)-[3-^{2}H]histidinol was synthesized by a stereochemically unambiguous route (Scheme 5).

The catalytic hydrogenation of **14** is the key step in the synthesis of (2*S**,3*S**)-[3-^{2}H]histidinol, since this step establishes the relative stereochemistry at carbons 2 and 3. While it can be assumed that catalytic hydrogenation involves a *syn* addition to the double bond, knowledge of the double bond configuration is critical. Accordingly, azlactone **13** was crystallized and its

Scheme 5

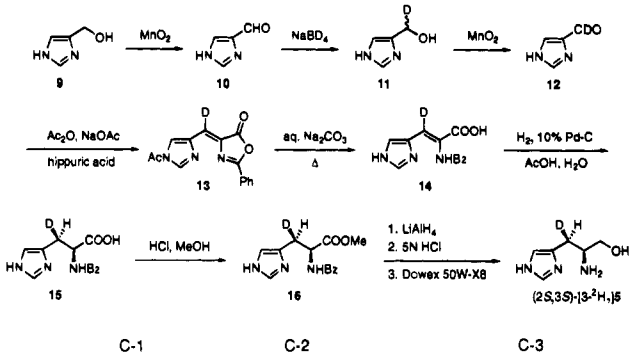

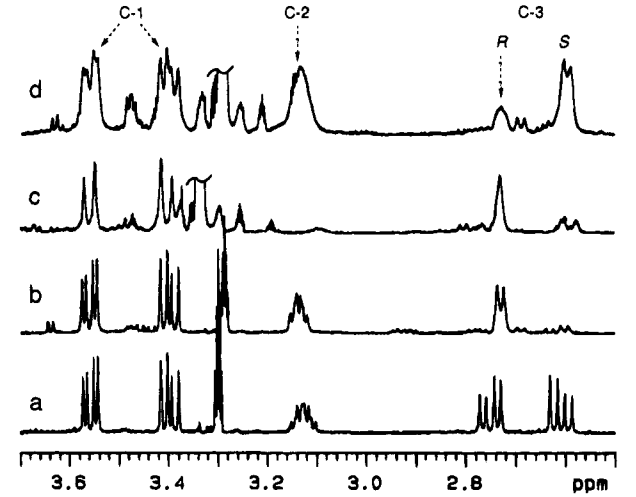

Figure 2. Alkyl side chain region of the ^{1}H NMR spectra (500 MHz) of ^{2}H-labeled and unlabeled histidinol (**5**) in CD_3OD: (a) unlabeled **5**; (b) synthetic (2*S**,3*S**)-[3-^{2}H]**5**; (c) (2*S*,3*S*)-[2,3-^{2}H]**5**, generated enzymatically from unlabeled IGP in D_2O; (d) (2*S*,3*R*)-[3-^{2}H]**5**, generated enzymatically from [3-^{2}H]IGP in H_2O.

structure determined by X-ray crystallography, The ORTEP drawing (supporting information) of **13** clearly indicates that the exocyclic double bond has the *Z* configuration, as shown in Scheme 5.

NMR Analysis of Labeled Histidinol Samples. In the ^{1}H NMR spectrum of unlabeled histidinol (spectrum a, Figure 2), the C-3 proton signals are seen as double doublets at 2.61 and 2.75 ppm. In the spectrum of synthetic (2*S**,3*S**)-[3-^{2}H]-histidinol (spectrum b), the higher-field C-3 proton resonance is missing, and the lower-field signal appears as a broadened doublet that is shifted slightly upfield, due to the deuterium isotope effect.[13] Thus, the lower- and higher-field C-3 signals of histidinol can be assigned to the *pro*-3*R* and *pro*-3*S* protons, respectively, Histidinol generated enzymatically from unlabeled IGP in D_2O (spectrum c) is labeled predominantly in the *pro*-3*S* position. In addition, the signal assigned to the C-2 proton, which exchanges during the transamination reaction, is missing. The complementary result is seen for [3-^{2}H]histidinol generated from [3-^{2}H]IGP in H_2O (spectrum d).

The ^{1}H NMR spectra (c and d in Figure 2) of both samples of enzymatically-generated, deuterium-labeled histidinol clearly indicate chiral labeling at C-3; however, the degree of stereoselectivity in the overall process is difficult to assess, due to overlapping signals from minor impurities, A much clearer answer was obtained from ^{2}H NMR analysis of the same samples (Figure 3).

The ^{2}H NMR spectrum of [2,3,3-^{2}H]histidinol is shown in Figure 3, spectrum d. The two C-3 deuteron resonances are well-resolved, and the assignments shown are consistent with

(10) Hawkes, T. R.; Thomas, P. G.; Edwards, L. S.; Rayner, S. J.; Wilkinson, K. W.; Rice, D. W. *Biochem. J.* **1995**, *306*, 385−397.
(11) Davisson, V. J.; Deras, I. L.; Hamilton, S. E.; Moore. L. L. *J. Org. Chem.* **1994**, *59*, 137−143.
(12) Klem, T. J.; Davisson, V. J. *Biochemistry* **1993**. *32*, 5177−5186.
(13) Hansen. P. E. *Annu. Rep. NMR Spectrosc.* **1983**, *15*, 105−234.

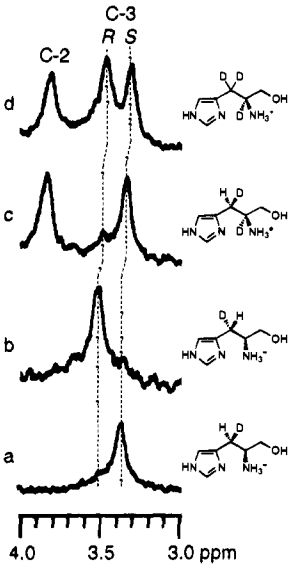

Figure 3. ^2H NMR spectra (76.728 MHz) of ^2H]-labeled histidinol (**5**) in CH_3OH: (a) synthetic (2*S**,3*S**)-[3-^2H]**5**; (b) (2*S*,3*R*)-[3-^2H]**5**, generated enzymatically from [3-^2H]IGP in H_2O; (c) (2*S*,3*S*)-[2,3-^2H]-**5**, generated enzymatically from unlabeled IGP in D_2O; (d) (2*S*)-[2,3,3-^2H]**5**, generated enzymatically from unlabeled IGP in D_2O, using minimal IAP aminotransferase and L-glutamate.The spectra are referenced to a $CDCl_3$ external standard.

the chemical shift of the single resonance in spectrum a, of synthetic (2*S**,3*S**)-[3-^2H]histidinol. (Note the deuterium-induced upfield shifts[13] in the multiply-labeled samples, as denoted by the dotted lines in Figure 3.) In the ^2H NMR spectrum of histidinol that was prepared enzymatically from [3-^2H]IGP in H_2O (Figure 3, spectrum b), a single resonance, for the *pro*-3*R* deuteron, is observed. Spectrum c of histidinol produced from unlabeled IGP in D_2O reveals two strong signals, one for the C-2 deuteron, and the other for deuterium in the *pro*-3*S* position. It is clear that the IGPD reaction is highly stereoselective (or stereospecific) and, on the basis of the (2*R*,3*S*) configuration of natural IGP, that the reaction proceeds with inversion of configuration.

Spectroscopic Analysis of IAP. NMR. At ambient probe temperature, IAP in D_2O exhibits two upfield doublets, at 3,66 and 4,49 ppm, and four resonances in the aromatic region, at 7.19, 7.23, 8.27, and 8.42 ppm. Each of the upfield resonances integrates to ca, 1H and is coupled to phosphorus, as shown by ^{31}P decoupling, Each of the aromatic resonances integrates to ca. 1H. Upon heating of the sample to 50 °C, the signals at 4.49, 7.19, and 8,42 ppm increase markedly in intensity, at the expense of the other three signals. The signals return to their original intensities when the sample is cooled to ambient temperature. Thus, in aqueous solution, IAP appears to be a mixture of two interconvertible compounds. In 90% H_2O, there are slight changes in the chemical shifts of the six resonances, and two additional upfield singlets are observed, at 3.04 and 4,02 ppm. (^1H and ^{13}C NMR spectra of IAP in H_2O and D_2O are included in the supporting information,) The integrals of the two most upfield aliphatic resonances are equal and somewhat less than the integrals of the other two aliphatic resonances, which are also equal to one another.

The ^{13}C NMR spectrum of IAP in D_2O was complicated by the presence of several resonances that appeared as doublets. At 60 °C, three of the resonances were diminished in intensity and the original signal ratios were reestablished upon cooling of the sample to ambient temperature. These observations are consistent with two interconvertible forms in solution, as had been suggested by the ^1H NMR data. In 90% H_2O, two

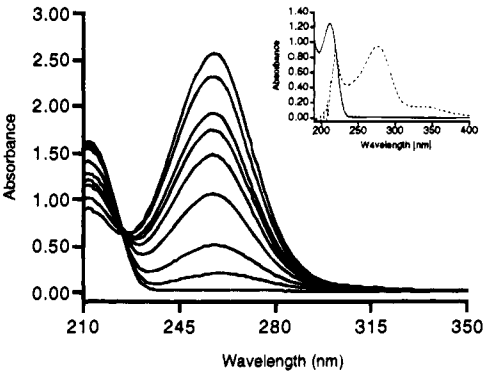

Figure 4. UV−vis spectra, demonstrating formation of the IAP−Mn^{2+} complex in ACES (20 mM, pH 6.1; 0.46 mM IAP, 0.8 mM $MnCl_2$). The sample was scanned every 30 s, but only selected scans are shown. The inset shows the UV−vis spectra of IAP (−) and the IAP enolate (- - -).

additional ^{13}C resonances were observed, at 34,6 and 32.5 ppm. An HMQC analysis showed correlation between the 34.6 and 32,5 ppm ^{13}C resonances and the rapidly exchangeable ^1H resonances at 3.04 and 4,02 ppm, respectively. These signals were assigned to the C-3 methylene protons, Assignments of the solution structures for IAP were based upon the temperature dependence of the NMR resonances and on the chemical shifts of the two ^{13}C signals for C-2, at 207,9 and 94.3 ppm. The downfield ^{13}C resonance is consistent with the ketone structure for IAP, while the second resonance at 94,3 ppm falls in the chemical shift range for ketone hydrates.[14] Shown below are the structure of the IAP hydrate and the NMR chemical shifts that support its existence along with the keto form:

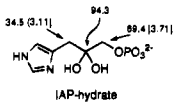

Spectroscopic Analyses of IAP−Mn^{2+}. IAP at 0.46 mM in ACES (20 mM, pH 6.1) has an absorption maximum at 212 nm. Under identical conditions, but in the presence of $MnCl_2$ (800 μM), the 212 nm absorption decreases while a new species with an absorption maximum at 257 nm forms (Figure 4). Addition of NaOH to the solution results in formation of the previously described IAP enolate,[15] In H_2O containing just Mn^{2+}, IAP forms a species with UV−vis characteristics identical to those described above for the ACES system. The rate of formation of the putative IAP−Mn^{2+} species is at least 5-fold greater in buffered solutions, across the pH range of 6.0−8.5, using a variety of organic bases such as Tris, HEPES, ACES, Bis-Tris propane, HEPPS, and triethanolamine (data not shown). EPR studies reveal that IAP forms a 1:1 chelation complex with Mn^{2+} (K_d = 250 μM) in HEPPS (20 mM, pH 8.1). The phosphate ester group of IAP appears to be critical for coordination with Mn^{2+}, since EPR spectroscopy shows that imidazoleacetol does not complex with Mn^{2+}. Similar measurements with the diol phosphate monoester IGP indicated a Mn^{2+} complex with K_d = 5.7 mM and no UV−vis absorption properties that are distinguishable from those of IGP, The altered absorption spectrum of IAP complexed to Mn^{2+} is reminiscent of, but not identical to, that of the IAP enolate, with the differences attributed to the coordination effects of a manganese ion (see below),

(14) Mackenzie, N. E.; Malthouse, P. G.; Scott, A. I. *Science* **1984**, *225*, 883−889.

(15) Ames, B. N.; Horecker, B. L. *J. Biol. Chem.* **1956**, *220*, 113−128.

Scheme 6

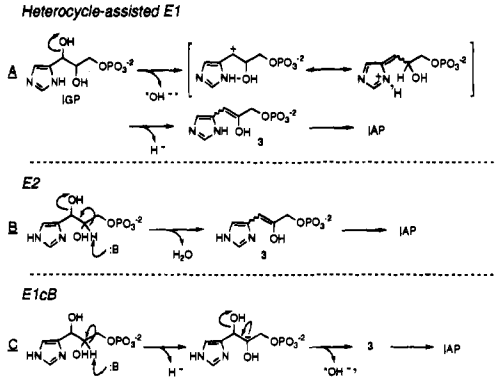

Discussion

Enzyme-catalyzed dehydrations are common biochemical events. In general, substrates for enzyme-catalyzed dehydrations have a proton and a hydroxyl group located α and β, respectively, to an electron-withdrawing moiety. An example of a substrate that lacks this functional group arrangement is IGP, the substrate for the IGPD reaction. Glycerol dehydrase and diol dehydrase also use vicinal diol substrates,[16] and this suggests that IGPD might share common mechanistic features with these enzymes. The reactions catalyzed by glycerol dehydrase and diol dehydrase require coenzyme B_{12}. The corrinoid cofactors of glycerol dehydrase and diol dehydrase are intimately involved in catalytic processes that are thought to proceed via radical mechanisms.[16] *E. coli* IGPD activity is not dependent upon coenzyme B_{12}, and the results described herein are not consistent with a radical mechanism of action. A coenzyme B_{12} *independent* diol dehydrase from the strict anaerobe *Clostridium glycolicum* is also thought to use a radical mediated process to catalyze the dehydration of 1,2-ethanediol and 1,2-propanediol.[17] Many unusual dehydrations that occur in strict anaerobes, such as clostridia, are catalyzed by enzymes that require cofactors other than coenzyme B_{12}.[18-21] *E. coli* IGPD requires only Mn^{2+} and 2-mercaptoethanol for optimal activity, and the reductant is proposed to simply prevent intra- and/or intersubunit disulfide bonds from forming during purification and storage of the enzyme, IGPD's Mn^{2+} cofactor may facilitate the catalytic process as it does for several other enzyme-catalyzed dehydrations which use metal ion cofactors as Lewis acids to activate leaving groups,[22-24] or to facilitate other steps in a given dehydration.[25,26]

Mechanisms hypothesized for the IGPD reaction are shown in Scheme 6. From a strict chemical perspective, mechanism A is the most attractive. It is essentially an E1 mechanism, with stabilization of the carbocation intermediate by the adjacent heterocycle. Analogous eliminations from (hydroxymethyl)-pyrroles are well-precedented,[27] Mechanisms B and C are less appealing, due to the high activation energy for deprotonation of an exceedingly weak carbon acid. In principle, however, complexation of the C-3 hydroxyl group with an electrophilic catalyst such as a metal ion could facilitate mechanism B. In this regard, it has been noted that β-eliminations from strong and weak carbon acids tend to occur with *syn* and *anti* steric courses, respectively,[28] and it is conceivable that those β-elimination substrates that are the weakest carbon acids (e.g., 10-hydroxystearate[29]) must react by concerted E2 mechanisms.

Scheme 7

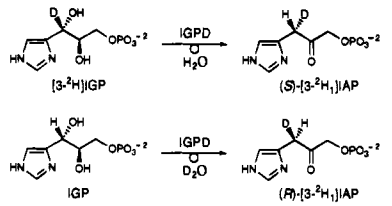

There are otherwise-plausible mechanisms for the IGPD reaction that can be eliminated from consideration at this time. As discussed above, other diol dehydrases appear to use cobalt cofactors, such as coenzyme B_{12}, to mediate radical reactions, and there are examples of pinacol rearrangements in secondary metabolism.[30-33] These reaction mechanisms, which are accompanied by intramolecular hydrogen transfer, involve radical or hydride intermediates, and thus are not consistent with the present results. Specifically, the "new" hydrogen at C-3 of IAP comes from the aqueous reaction medium, since IGPD converts unlabeled IGP to [3-^{2}H]IAP when the reaction is run in D_2O (Scheme 7).

The results of this study establish that the IGPD reaction is highly stereoselective (or stereospecific) and, specifically, that it proceeds with inversion of configuration (Scheme 7). The fact that the reaction is stereoselective indicates that *enol 3 is a likely reaction intermediate, and that its tautomerization to IAP (2) must be enzyme-catalyzed, rather than occurring spontaneously in solution.* While the stereoselectivity of the IGPD reaction is readily interpretable, the significance of the fact that the reaction occurs with inversion (rather than retention) of configuration at C-3 remains unknown. The full interpretation of this result will require further information regarding the stereochemistry of the reactive intermediate(s) and additional studies of the enzyme itself,

Solution Chemistry of IAP. While the stereochemical results described in this paper are clear and unequivocal, they were obtained only after optimization of the coupled enzyme system (Scheme 2). In fact, in early experiments with the coupled enzyme system, chirality at C-3 was lost. Specifically, incubation of [3-^{2}H]IGP with IGPD in H_2O and of unlabeled IGP with IGPD in D_2O led to the isolation of unlabeled histidinol and [2,3,3-^{2}H]histidinol, respectively. Since the coupled enzyme system had been devised to minimize exchange

(16) Toraya, T. In *Metal Ions in Biological Systems*; Sigel, H., Sigel, A., Eds.; Marcel Dekker. Inc.: New York, 1994: Vol. 30, pp 217–254.
(17) Hartmanis, M. G. N. In *Metal Ions in Biological Systems*; Sigel, H., Sigel, A., Eds.; Marcel Dekker, Inc.: New York 1994; Vol. 30, pp 201–215.
(18) Buckel, W. *FEMS Microbiol. Rev.* **1992**, *88*, 211–232.
(19) Scherf, U.; Buckel, W. *Eur. J. Biochem.* **1993**, *215*, 421–429.
(20) Klees, A.-G.; Linder, D.; Buckel, W. *Arch. Microbiol.* **1992**, *158*, 294–301.
(21) Hofmeister, A. E. M.; Buckel, W. *Eur. J. Biochem.* **1992**, *206*, 547–552.
(22) Villafranca, J. J.; Nowak, T. In *The Enzymes*, 3rd ed.; Boyer, P. D., Ed.; Academic Press: New York, 1992; Vol. 20, pp 63–94.
(23) Kennedy, M. C.; Stout, C. D. *Adv. Inorg. Chem.* **1992**, *38*, 323–339.
(24) Schweiger, G.; Dutscho, R.; Buckel, W. *Eur. J. Biochem.* **1987**, *169*, 441–448.
(25) Jordan, P. M. In *New Comprehensive Biochemistry: Biosynthesis of Tetrapyrroles*; Jordan, P. M., Ed.; Elsevier: New York, 1991; Vol. 19, pp 1–59.
(26) Jaffe, E. K.; Abrams, W. R.; Kaempfen, H. X.; Harris, K. A., Jr. *Biochemistry* **1992**, *31*, 2113–2123.
(27) Katritzky, A. R. *Handbook of Heterocyclic Chemistry*; Pergamon Press: Oxford, 1985.
(28) Widlanski, T.; Bender, S. L.; Knowles, J. R. *Biochemistry* **1989**, *28*, 7572–7582.
(29) Schroepfer, G. J., Jr. *J. Biol. Chem.* **1966**, *241*, 5441–5447.
(30) Frey, P. A.; Moss, M.; Petrovich, R.; Baraniak, J. *Ann. N. Y. Acad. Sci.* **1990**, *585*, 368–378.
(31) Ballinger, M. D.; Frey, P. A.; Reed, G. H. *Biochemistry* **1992**, *31*, 10782–10789.
(32) Scott, A. I.; Wiesner, K. J. *J. Chem. Soc., Chem. Commun.* **1972**, 1075–1077.
(33) Volk, R.; Bacher, A. *J. Biol. Chem.* **1991**, *266*, 20610–20618.

of IAP, we considered the possibility that exchange of the these protons might result from normal mechanistic events catalyzed by the two enzymes. In particular, IGPD might stereospecifically introduce a solvent proton at C-3, and the aminotransferase might exchange the remaining C-3 proton. However, control experiments designed to detect solvent exchange in the back-reaction failed to implicate the aminotransferase in the solvent exchange, and this led to a more detailed characterization of IAP. Only limited spectroscopic analyses of IAP had been conducted prior to the current study. An original key discovery[15] was that both IAP and imidazoleacetol, when treated with base, give species with unique, long-wavelength electronic absorptions, which serve as the basis of a useful end point assay for IGPD activity. This observation was attributed logically to the formation of the IAP enolate by removal of a C-3 proton.

In aqueous solution under all conditions examined in the current study, IAP undergoes rapid exchange of its C-3 protons, as detected by NMR spectroscopy. This characteristic can be understood by considering intramolecular interactions that can exist in IAP but not in the analog dihydroxyacetone phosphate. (The α protons of DHAP do not exchange when incubated in tritiated water at 37 °C for 3 h,[34] and we observe that the α protons of DHAP do not exchange even after incubation in D_2O at 4 °C for 4 weeks (data not shown).) At pH values around neutrality, a significant proportion of the imidazole ring of IAP must exist in the imidazolium form. One possible explanation for the lability of the C-3 protons of IAP is that an intramolecular hydrogen bond is formed between $N^{\delta 1\text{-}H}$ of the imidazole ring and the carbonyl group at C-2 of IAP (IAP*). This type of

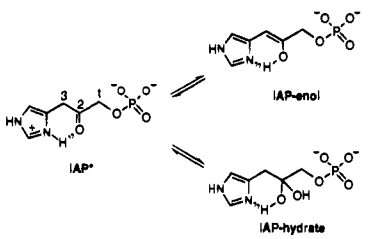

intramolecular hydrogen bonding polarizes the carbonyl bond, increasing the electrophilic character of C-2, and therefore the acidity of the protons at C-3. Formation of an IAP enol ultimately results in exchange of the C-3 protons with bulk solvent as a reversible equilibrium occurs between the keto and enol species. These interactions may also help to explain the facile formation of the IAP hydrate. Alternatively, intramolecular hydrogen bonding with the phosphate oxygens could stabilize the IAP hydrate and allow for its detection by NMR spectroscopy.

Additional solution chemistry of IAP in the presence of Mn^{2+} was analyzed by UV−vis and EPR spectroscopy. The formation of an IAP−Mn^{2+} complex appears to be buffer-catalyzed, and UV−vis absorption properties of the complex are distinct from those of IAP or the IAP enolate (Figure 4). EPR titration experiments confirm that IAP coordinates to Mn^{2+} with a 1:1 stoichiometry and that the phosphate ester group is essential for the interaction. The high affinity of IAP for Mn^{2+} distinguishes the IAP−Mn^{2+} complex from a simple monodentate phosphate monoester coordination complex.[35] Furthermore, the interactions appear unique to IAP, since the IGP−Mn^{2+} complex has a K_d typical of a phosphate monoester−Mn^{2+} complex, and no shifts are observed in the UV−vis spectrum.

(34) Rieder, S. V.; Rose, I. A. *J. Biol. Chem.* **1959**, *234*, 1007−1010.
(35) Cohn, M.; Townsend, J. *Nature* **1954**, *173*, 1090−1091.

Mildvan and co-workers have studied similar chemistry involving Mn^{2+} complexes of acetol phosphate (AP) and DHAP.[36] In contrast to our finding, they observed that a *monodentate* coordination complex is formed in aqueous solutions between $Mn^{2+}$and the phosphoryl group of AP. However, proton relaxation studies gave results suggesting that when it is bound to the enzyme aldolase, DHAP (the C-3-hydroxylated analog of AP) forms a bidentate complex with Mn^{2+}, via coordination to the phosphoryl group and the carbonyl oxygen.[36] The results of additional model studies by Sigel and co-workers[37] are consistent with the idea that the tendency toward bidentate metal−ligand interaction may be enhanced in a sequestered enzyme active site. They observed a seven-membered cyclic chelate between Cu^{2+} and the phosphate and carbonyl of DHAP in aqueous dioxane, a system they propose mimics the environment of an enzyme active site. In either case, the effective dielectric constant, relative to bulk solvent, is reduced, presumably favoring the formation of chelates.[37]

Clearly, the imidazole moiety is intimately involved in the unique solution-phase coordination chemistry of IAP. We propose that the substantial red shift that is observed in the UV spectrum of IAP in the presence of Mn^{2+} (Figure 4) reflects the formation of a metal−*enolate* coordination complex and that the enolate oxygen is a stronger ligand than is the carbonyl oxygen. This proposal is supported by IAP's much greater tendency than AP or DHAP toward α-deprotonation, due to the involvement of the imidazole ring in resonance stabilization of the C-3 carbanion and the fact that the enolate has an extended π-system. An IAP enolate−Mn^{2+} complex could be either bidentate or tridentate. In the latter case, $N^{\delta 1}$ of the imidazole could serve as the third ligand.

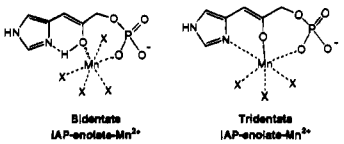

The potential biological significance of the IAP solution chemistry lies in IGPD's metal ion cofactor requirement for catalytic turnover. On the basis of the fact that an IAP−Mn^{2+} complex is observed in aqueous solution, it is reasonable to suggest that similar interactions are relevant to binding and catalysis at the enzyme's active site. The results described in this paper are consistent with the IGPD reaction proceeding through an enol intermediate, **3** (Scheme 6). The role of Mn^{2+} may extend beyond binding of the substrate to promoting the formation of an IAP enol−Mn^{2+} complex through direct coordination of the C-2 oxygen. Although the solution data cannot define the exact role(s) of the metal ion cofactor in IGPD, the results presented herein are certainly provocative and provide a framework for more detailed investigations of the coordination chemistry involving the metal, the protein, and the bound forms of the substrate and product.

Experimental Section

Chemical Materials and Methods. $NaBD_4$ was purchased from MSD Isotopes. THF and Et_2O were distilled from $LiAlH_4$, under nitrogen, prior to use. Benzene was distilled from benzophenone ketyl, under nitrogen. CH_3CN, MeOH, and pyridine were distilled from CaH_2. Ac_2O and $POCl_3$ were distilled freshly prior to use. $CHCl_3$ was washed with H_2O to remove EtOH, dried with $CaCl_2$, and filtered to remove

(36) Mildvan, A. S. *Advances in Chemistry Series*; American Chemical Society: Washington, DC, 1971; Vol. 100, pp 390−412.
(37) Liang, G.; Chen, D.; Bastian, M.; Sigel, H. *J. Am. Chem. Soc.* **1992**, *114*, 7780−7785.

the drying reagent. All other chemicals were reagent grade and were purchased from Aldrich or Sigma. Flash chromatography[38] was performed on silica gel 60, 230–400 mesh (EM Science), and silica gel GHLF plates (Analtech) routinely were used for thin layer chromatography. TLC plates were visualized with ultraviolet light, I_2 vapor, or ethanolic phosphomolybdic acid. Avicel F cellulose plates (250 μm) were obtained from Analtech. NMR spectra were obtained on a Chemagnetics A-200, Brüker ARX 300, or Varian VXR-500 NMR spectrometer. ^{1}H chemical shifts are internally referenced to residual solvent lines or to added 3-(trimethylsilyl)propionic-*2,2,3,3-d*$_4$ acid sodium salt (0.0 ppm) in ^2H_2O. ^{2}H NMR spectra are referenced to deuterium at natural abundance in $CHCl_3$ (7.28 ppm) in a 5 mm glass insert within a 10 mm tube containing the sample in MeOH. ^{13}C NMR spectra are referenced to external dioxane (66,5 ppm). ^{31}P NMR spectra are referenced to external concentrated H_3PO_4 (0.0 ppm). Infrared spectra were obtained on a Perkin-Elmer Model 1600 Fourier transform infrared spectrophotometer. CI (isobutane) mass spectra were obtained through the Purdue University Department of Medicinal Chemistry and Pharmacognosy Mass Spectrometry Laboratory, with a Finnigan 4000 quadrupole mass spectrometer. UV–vis spectra were collected on a Varian Cary 3 spectrophotometer. EPR spectra were measured on a Varian E-Line Century Series EPR spectrometer. X-ray crystallographic data were obtained and analyzed by Pascal Toma in the Purdue University Department of Chemistry X-ray Crystallography Laboratory, using an Enraf-Nonius CAD4 computer-controlled κ axis diffractometer equipped with a graphite crystal, incident beam monochromator. The structure was solved using the program SHELX-86.[39]

General Biochemical Materials and Methods. Oligonucleotide primers used in polymerase chain reactions (PCR) were obtained from the Laboratory Center for Macromolecular Structure at Purdue University and purified by polyacrylamide gel electrophoresis (PAGE).[40] Pyrophosphatase was purchased from United States Biochemical, and [α-^{35}S]dATP was purchased from Amersham. Isopropyl β-D-glucopyranoside (IPTG) was purchased from Gold Biotechnology, Glutamate dehydrogenase and dNTPs were purchased from Boehringer-Mannheim. Plasmids pVG-2 and pJF119EH were provided by the laboratories of C. Bruni and E. Lanke, respectively. Restriction enzymes were purchased from New England Biolabs or Stratagene. *E. coli* XL-1 Blue and pBluescript II SK+ were purchased from Stratagene. The GeneClean kit was purchased from Bio101, Inc., and T4 DNA ligase and *Taq* DNA polymerase were from Promega. DNA sequencing was carried out by the dideoxynucleotide method using the Sequenase kit, version 2.0 (United States Biochemical). All sequencing reactions contained [α-^{35}S]dATP (5 μCi) and pyrophosphatase (0.004 unit) to eliminate variations in band intensity; when elimination of band compressions was necessary, 7-deaza-GTP was substituted for dGTP.[41] Sequencing reactions were analyzed on 8% polyacrylamide/6.8 M urea gels, which were dried and used to expose to Kodak X-OMAT AR film for 12–24 h at ambient temperature. Protein PAGE was carried out on 10% acrylamide gels according to the method of Laemmli.[42] Protein was visualized by staining the gels with Coomassie Brilliant Blue R-250. The concentrations of protein solutions were determined by the method of Bradford[43] using the Bio-Rad kit with bovine serum albumin as the standard. Centriprep 10 concentration units were purchased from Amicon. *E. coli* PRPP synthetase was from Sigma and *E. coli* strains overexpressing histidine biosynthetic enzymes other than HisB and HisC were previously described.[11] Densitometry scans were carried out using a Shimadzu CS 9000U dual wavelength flying spot scanner.

Construction of *phisB-tac*. A 1070-bp DNA fragment containing the *hisB* gene was amplified from the vector pVG-2,[44] which contains the distal portion of the histidine operon (*hisBHAFIE*), via PCR using a sense primer (5′-CGGAATTCAT**ATG**AGTCAGAAGTATCTTTT-3′) containing an overlapping *Eco*RI/*Nde* I site and an antisense primer (5′-CGGGATCC**TCATTA**CAGCACTCCTTTCGAC-3′) containing a *Bam*HI site. (The restriction sites are underlined, and start and stop codons are shown in bold face type.) The PCR was run for 26 cycles with an initial cycle of 3 min at 93 °C, 2 min at 37 °C, and 2 min at 72 °C, and 25 subsequent cycles of 1 min at 93 °C, 2 min at 37 °C, and 2 min at 72 °C. The PCR mixture (100 μL) contained dNTPs (0.2 mM each), primers (700 pmol each), a template (10 ng), $MgCl_2$ (2.5 mM), *Taq* DNA polymerase (5 U), and *Taq* DNA polymerase buffer (1× final concentration). The reaction was overlaid with 100 μL of light mineral oil. Following electrophoretic purification, the DNA generated by PCR was extracted from a 0.7% agarose gel using the GeneClean kit, digested with *Bam*HI and *Eco*RI, and cloned into pBluescript II SK+ at the *Bam*HI and *Eco*RI sites using T4 DNA ligase, to give pBluescript-*hisB*. Recombinants were selected from transformed *E. coli* XL-1 Blue on LB plates supplemented with ampicillin (Ap) (50 μg/mL) and tetracycline (Tc) (15 μg/mL). Colonies were grown in 4 mL of 2xYT liquid medium containing Ap (50 μg/mL) and Tc (15 μg/mL) overnight at 37 °C and plasmid DNA was isolated from these cultures using the alkaline lysis method.[45] Both strands of the *hisB* insert in this construct were sequenced to confirm that *hisB* had been amplified and cloned without mutation. The *hisB* insert was isolated from pBluescript-*hisB* and cloned into pJF119EH,[6] at the *Eco*RI and *Bam*HI sites, to yield p*hisB-tac* after isolation as described above. The p*hisB-tac* construct was transformed into *E. coli* FB 251 (a *hisB* mutant strain). The ability of the transformants to grow on a histidine deficient medium[46] indicated that a functional *hisB* had been supplied to the mutant strain. The strain for high-level HisB production, *E. coli* FB1-*hisB*, was made using p*hisB-tac* to transform *E. coli* FB1 (a histidine operon deletion mutant).

Production of IGPD. Production of *E. coli* IGPD was demonstrated by growing a colony of *E. coli* FB1-*hisB* in 4 mL of 2xYT (100 μg/mL Ap) for 12 h at 37 °C. Two hundred microliters of this culture was used to inoculate 25 mL of fresh medium. Cells were grown to OD_{550} = 1.0, and expression of *hisB* was induced by adding IPTG to a final concentration of 1 mM. Samples suitable for analysis by 10% SDS–PAGE (Figure 1) were prepared from 1 mL aliquots taken at 0, 2, 4, 6, and 8 h. Cells were harvested by centrifugation, and the pellets were lysed by resuspension in 0.1 mL of H_2O and 0.1 mL of 2× SDS sample buffer before heating at 100 °C for 6 min,[39] and removal of cell debris by centrifugation. One liter cultures were grown under the same conditions and harvested after 6–8 h. For extraction of active IGPD, the cell paste from a 25 mL culture was resuspended in 2 mL of buffer containing 100 mM triethanolamine (pH 8.1), 85 mM 2-mercaptoethanol, and 200 μM $MgCl_2$. The cells were lysed by ultrasonication, and the cell debris was removed by centrifugation. Typical preparations contained protein at 5–10 mg/mL and showed IGPD specific activities of 10–12 U/mg.

Construction of *phisC-tac*. A 1063-bp fragment of DNA containing *hisC* was amplified from the vector pHC9800[44] using the same protocols as described previously for *hisB*. The sense primer (5′-CGGAATTCAT**ATG**AGCACCGTGACTATTAC-3′) incorporated an *Eco*RI/*Nde*I site, and the antisense primer (5′-CGGGATCC**TCATCA**AACTTGCTCCGCACGT-3′) incorporated a *Bam*HI site. The PCR product was cloned into pBluescript II SK+ at the *Eco*RI and *Bam*HI sites and transformed into *E. coli* XL-1 Blue to yield *E. coli* XL-1-*hisC*. *hisC* was isolated from this construct and cloned into pJF119EH[6] at the *Eco*RI and *Bam*HI sites to yield p*hisC-tac*. *E. coli* UTH 780, a *hisC* mutant strain (*E. coli* Genetic Stock Center, Yale University), grew on histdine deficient medium[46] when transformed with p*hisC-tac*, indicating that a functional HisC was produced from the plasmid. The p*hisC-tac* construct was transformed into *E. coli* FB1, and the *hisC* expression strain was designated *E. coli* FB1-*hisC*.

(38) Still, W. C.; Kahn, M.; Mitra, A. *J. Org. Chem.* **1978**, *43*, 2923–2925.
(39) Sheldrick, G. M. Ph.D. Thesis, Universität Göttingen, 1986.
(40) Ausubel, F. M.; Brent, R.; Kingston, R. E.; Moore, D. D.; Seidman, J. G.; Smith, J. A.; Struhl, K. *Current Protocols in Molecular Biology*; Greene Publishing and Associates and John Wiley & Sons: New York, 1993.
(41) Mizusawa, S.; Nishimura, S.; Seela, F. *Nucl. Acids Res.* **1986**, *14*, 1319–1324.
(42) Laemmli, U. K. *Nature* **1970**, *227*, 680–685.
(43) Bradford, M. M. *Anal. Biochem.* **1976**, *72*, 248–254.
(44) Carlomagno, M. S.; Chiariotti, L.; Alifano, P.; Nappo, A. G.; Bruni, C. B. *J. Mol. Biol.* **1988**, *203*, 585–606.
(45) Maniatis, T.; Fritsch, E. F.; Sambrook, J. *Molecular Cloning: A Laboratory Manual*; Cold Spring Harbor Laboratory Press: Cold Spring Harbor, NY, 1982.
(46) Vogel, H. J.; Bonner, D. M. *J. Biol. Chem.* **1956**, *218*, 97–106.

Production and Purification of IAP Aminotransferase. SDS-PAGE analysis of IAP aminotransferase production in *E. coli* FB1-*hisC* was carried out as described for IGPD (Figure 1). For purification on a large scale, *E. coli* FB1-*hisC* was grown to OD_{550} = 1.0, and expression of *hisC* was induced by adding IPTG (Gold Biotechnology) to a final concentration of 1 mM. After an additional 8 h of growth, the cells were harvested by centrifugation and stored at −80 °C. IAP aminotransferase has been purified previously from *Salmonella typhimurium*.[47] However, with this efficient production system, a simplified purification protocol was used. For a typical preparation, 6 g of frozen *E. coli* FB1-*hisC* was thawed in HEPPS (20 mM, pH 8.1; buffer A) at 45 °C over 10 min. Cells were disrupted by two passes through a French pressure cell (Amicon) at 15 000 psi, and the cell debris was removed by centrifugation at 27 000*g* for 15 min. Nucleic acids were precipitated from the supernatant by addition of 10% (w/v) streptomycin sulfate in buffer A to a final concentration of 1% (w/v) and centrifugation at 27 000*g* for 15 min. The nucleic acid-free supernatant was applied to a 2.5 cm × 15 cm Q-Sepharose column, equilibrated in buffer A. IAP aminotransferase activity eluted at ca. 250 mM NaCl in an 800 mL linear gradient of 0−1 *M* NaCl in buffer A. Fractions (8.1 mL) were collected at 2 mL/min, and those fractions with IAP aminotransferase activity, 7 U/mg or greater, were pooled. Precipitated IAP aminotransferase was isolated by centrifugation of the 20−40% $(NH_4)_2SO_4$ fraction at 12 000*g* for 10 min. The pellet was resuspended in 4 mL of buffer A and loaded onto a 2.5 cm × 81 cm Sepharose S-400 column (Pharmacia). Fractions (8.1 mL) were collected at 1 mL/min, and those with IAP aminotransferase activity of at least 10 U/mg were collected, pooled, and concentrated to 30 mg/mL using an Amicon stirred ultrafiltration cell equipped with a PM-10 filter. Purified IAP aminotransferase was stored in 50% glycerol at −20 °C.

Coupled Assay for IGPD Activity. A 200-fold unit excess of IAP aminotransferase and a 500-fold unit excess of glutamate dehydrogenase (Boehringer-Mannheim) relative to IGPD were utilized. Typically, a 1 mL assay included IAP aminotransferase (2.1 U) pre-incubated with 10 μL of a 0.5 mg/mL solution of pyridoxal phosphate, L-glutamate (10 mM), glutamate dehydrogenase (ca. 6 U), and NADH (0.01 mM). The assay buffer was HEPPS pH 8.1, containing 200 μM $MnCl_2$, 85 mM 2-mercaptoethanol, and 20 mM $(NH_4)_2SO_4$. All solutions were prepared immediately before use, and either IGP (2 mM final concentration) or IGPD (0.5 μg; 0.01 unit) was used to initiate the reaction.

1,2-*O*-Isopropylidene-α-D-[3-^{2}H]allofuranose (7). Compound **7** was prepared by the selective deprotection method of Reichman *et al.*[48] A solution of 1,2:5,6-di-*O*-isopropylidene-α-D-[3-^{2}H]allofuranose (4.58 g, 17.5 mmol), prepared from commercial diacetone-D-glucose (**6**) by the method of Baker *et al.*,[49] in 1:1 MeOH/0.7% aqueous H_2SO_4 was stirred at room temperature for 22 h. After neutralization with solid $BaCO_3$, the reaction mixture was boiled for 10 min. The resultant precipitate was removed by filtration under vacuum, and the filtrate was concentrated *in vacuo*, to a syrupy residue. A white solid was obtained after repeated addition of benzene and concentration *in vacuo* (3.50 g, 90%): mp 131−132 °C (for material recrystallized from EtOH, lit.[50] mp 128−129 °C); ^{1}H NMR (500 MHz, $CDCl_3$) δ 1.38 (s, 3 H, CH_3), 1.60 (s, 3 H, CH_3), 2.51 (d, *J* = 3.7 Hz, 1 H, C-5 OH), 2.59 (t, *J* = 6.5 Hz, 1 H, C-6 OH), 3.23 (s, 1 H, C-3 OH), 3.80 (m, 1 H, C-6), 3.88 (m, 2 H, C-6 and C-4), 4.05 (m, 1 H, C-5), 4.64 (d, *J* = 3.8 Hz, 1 H, C-2), 5.83 (d, *J* = 3.8 Hz, 1 H, C-1); IR (KBr pellet) 3352 (br), 2974, 2931, 2898, 2878, 1095, 1076, 1048, 874, 708 cm^{-1}.

1,2-*O*-Isopropylidene-α-D-[3-^{2}H]ribofuranose (8a). Compound **8a** was prepared by oxidative cleavage of C-6 and reduction with $NaBH_4$.[51] To a solution of **7** (3.30 g, 14.9 mmol) in H_2O (58 mL) at 0 °C was added $NaIO_4$ (4.55 g, 21.3 mmol). After 10 min, absolute EtOH (117 mL) was added, and the precipitated $NaIO_3$ was removed by filtration under vacuum. The filtrate was cooled to 0 °C, and solid $NaBH_4$ (1.13 g, 29.9 mmol) was added. After the solution had been stirred for 15 min at 0 °C and for 2.5 h at room temperature, the pH was adjusted to 7 with acetic acid, and EtOH was removed *in vacuo*. The residual liquid was saturated with solid NaCl and extracted eight times with CH_2Cl_2. The combined organic extracts were dried with Na_2SO_4 and filtered to remove the drying agent, and the filtrate was concentrated *in vacuo* to a slowly crystallizing white solid (1.42 g, 50%): mp 90−91 °C (for material recrystallized from Et_2O, lit.[51] mp 86−87 °C); ^{1}H NMR (500 MHz, $CDCl_3$) δ 1.38 (s, 3 H, CH_3), 1.58 (s, 3 H, CH_3), 2.20 (br s, 2 H, OH), 3.76 (dd, *J* = 12.4, 3.8 Hz, 1 H, C-5), 3.84 (dd, *J* = 3.8, 2.7 Hz, 1 H, C-4), 3.96 (dd, *J* = 12.4, 2.7 Hz, 1 H, C-5), 4.59 (d, *J* = 3.8 Hz, 1 H, C-2), 5.83 (d, *J* = 3.8 Hz, 1 H, C-1); IR (KBr pellet) 3347 (br), 2993, 2958, 2924, 2888, 1117, 1013, 876 cm^{-1}.

[3-^{2}H]-D-Ribose-5-phosphate (8b). Compound **8a** was phosphorylated by the method of Gross *et al.*[52] CH_3CN (2.6 mL) and freshly distilled $POCl_3$ (0.73 mL, 7.33 mmol) were combined in a dry 25 mL three-necked round bottom flask equipped with a thermometer. The resulting solution was stirred and cooled in an ice−salt bath, and pyridine (0.43 mL, 5.23 mmol) was injected dropwise over a period of 10 min. 1,2-*O*-Isopropylidene-α-D-[3-^{2}H]ribofuranose (**8a**) (1.0 g, 5.23 mmol) in CH_3CN (3.1 mL) was then injected dropwise into the mixture while the reaction temperature was maintained at ≤0 °C. The reaction mixture was allowed to stir at 0 °C for an additional 2 h and then poured into ice−water (21 mL) and heated at 70 °C for 1 h. The mixture was cooled in an ice bath, and the pH was adjusted to 5.0 with 10 N NaOH. Saturated aqueous $BaCl_2$ (5.2 mL) was added, and the resulting precipitate was removed by centrifugation. The supernatant was cooled to 0 °C, and the pH was adjusted to 7.5 with 10 N NaOH. Any solids were removed by filtration under vacuum, and to the cold filtrate was added EtOH (1.5 volumes). The resulting precipitate, the barium salt of [3-^{2}H]-D-ribose-5-phosphate (**8b**), was isolated by vacuum filtration, washed with EtOH, and dried *in vacuo* (1.01 g, 53%): ^{31}P NMR (202 MHz, D_2O) δ 4.21; FAB MS (Gly) *m/z* 230.

(2*R*,3*S*)-[3-^{2}H]Imidazoleglycerol Phosphate. [3-^{2}H]-D-Ribose-5-phosphate (**8b**) 160 mg, 428 μmol) was converted to 5-phospho-D-[3-^{2}H]-D-ribosyl-α-1-pyrophosphate ([3-^{2}H]PRPP) with PRPP synthetase by the method of Whitesides and co-workers.[52] Extracts from an *E. coli* strain overproducing HisG and HisIE were used to convert [3-^{2}H]PRPP to N^1-[(5″-phospho-β-D-[3-^{2}H]ribosyl)formimino]-5-aminoimidazole-4-carboxamide ribonucleotide (5′-[3-^{2}H]ProFAR),[8] which was purified on a 2.5 cm × 14 cm Q-Sepharose column (Pharmacia, HCO_3^- form). 5′-[3-^{2}H]ProFAR eluted at ca. 170 mM in a 1 L linear gradient from 0 to 250 mM NH_4HCO_3, and the appropriate pooled fractions were dried by lyophilization. The recovered 5′-[3-^{2}H]ProFAR was converted to [3-^{2}H]IGP by dissolving with Tris (100 mM, pH 7.5) containing $MgCl_2$ (30 mM), ATP (200 mg, 0.36 mmol), PEP (60 mg, 0.26 mmol), glutamine (200 mg, 1.37 mmol), and pyruvate kinase (56 U, 111 μg) in a total volume of 50 mL, and the pH was adjusted to 7.5 with 20 μL of 5 N NaOH. To this mixture was added purified HisA (5 U, 200 μg) and HisH/F (4 U, 400 μg). After incubating at 30 °C for 12 h, the mixture was loaded onto a 4.5 cm × 15 cm Dowex 1-X8 column (200−400 mesh, acetate form). The column was washed with H_2O, and then [3-^{2}H]IGP was eluted with 0.1 N HCl. Aliquots were spotted onto Avicel F cellulose TLC plates and sprayed with diazotized sulfanilic acid reagent.[53] [3-^{2}H]IGP was visualized as yellow spots on a white background, and the positive fractions containing IGP were pooled and dried by lyophilization. The yield of [3-^{2}H]IGP (32 mg) was 30%, based on [3-^{2}H]ribose-5-phosphate: UV−vis λ_{max} (H_2O) 215 nm (ε = 4500); ^{1}H NMR (500 MHz, D_2O) δ 3.91 (m, 1 H, C-1), 3.99 (m, 1 H, C-1), 4.06 (m, 1 H, C-2), 7.45 (d, *J* = 1.4 Hz, 1 H, imidazole 4(5)H), 8.57 (d, *J* = 1.4 Hz, 1 H, imidazole 2H); ^{13}C NMR (125 MHz, D_2O) δ 64.94 (d, $^3J_{CP}$ = 5.2 Hz, C-2), 72.01 (d, $^2J_{CP}$ = 7.6 Hz, C-1), 116.64, 132.54, 133.54, the signal to noise ratio was not appropriate to identify the triplet for C3; FAB HRMS (DTT/DTE) *m/z* calcd 238.0339, found 238.0318.

Enzyme-Catalyzed Conversion of (2*R*,3*S*)-IGP to [2,3-$^2H_2$]-Histidinol. IGP (11.5 mg, 48.5 μmol) was incubated with HisB-

(47) Martin, R. G.; Goldberger, R. F. *J. Biol. Chem.* **1967**, *242*, 1168−1174.

(48) Reichman, U.; Watanabe, K. A.; Fox, J. J. *Carbohydr. Res.* **1975**, *42*, 233−240.

(49) Baker, D. C.; Horton, D.; Tindall, C. G., Jr. *Methods Carbohydr. Chem.* **1976**, *7*, 3−6.

(50) Kiss, J.; D'Souza, R.; Taschner, P. *Helv. Chim. Acta* **1975**, *58*, 311−317.

(51) LeCocq, J.; Ballou, C. E. *Biochemistry* **1964**, *3*, 976−980.

(52) Gross, A.; Abril, O.; Lewis, J. M.; Geresh, S.; Whitesides, G. M. *J. Am. Chem. Soc.* **1983**, *105*, 7428−7435.

(53) Ames, B. N.; Mitchell, H. K. *J. Am. Chem. Soc.* **1952**, *74*, 252−253.

containing extract (ca. 13 U, 1.3 mg of protein in 3.5 mL of 100 mM triethanolamine/D_2O), HisC-containing extract (270 U, 27 mg of protein in 1.8 mL of 100 mM triethanolamine/D_2O), PLP (3 mg 12 μmol), and L-glutamate (2.14 g 12.7 mmol) in triethanolamine/D_2O (100 mM) in a total volume of 6.3 mL (pH 7.7, pD 8.1) in a 50 mL Falcon tube at 37 °C, in the absence of light for 2.5 h. The pH was monitored at 20 min intervals and adjusted to 7.7 as needed with 100 mM triethanolamine base. Histidinol was isolated by loading the mixture onto a 2.5 cm × 7 cm Dowex 50W-X8 column (200–400 mesh, NH_4^+ form) and eluting with a NH_4HCO_3/NH_4OH step gradient from pH 8.0 to pH 10.5 in 0.5 pH unit increments (10 mL per step). Aliquots were spotted onto Avicel F cellulose TLC plates and sprayed with diazotized sulfanilic acid reagent. Histidinol was visualized as yellow spots on a white background.[53] Fractions from the pH 10.5 wash that contained histidinol were pooled and lyophilized to dryness.

Enzyme-Catalyzed Conversion of (2*R*,3*S*)-IGP to [2,3,3-^{2}H]-Histidinol. IGP was converted to [2,3,3-^{2}H]histidinol using essentially the same methodology as for the conversion of (2*R*,3*S*)-IGP to [2,3-^{2}H]histidinol. In addition to unlabeled IGP (10 mg, 42 μmol), the incubation mixture included the HisB extract (300 μg of protein), HisC-containing extract (350 μg of protein), L-glutamate (28.5 mg, 169 μmol), and PLP (1.1 mg, 4.4 μmol). The reaction mixture was incubated at 37 °C for a period of 23 h. Following purification by ion exchange chromatography, the product (10.5 mg) was analyzed by ^{1}H and ^{2}H NMR.

Enzyme-Catalyzed Conversion of (2*R*,3*S*)-[3-^{2}H]IGP to [3-^{2}H]-Histidinol. [3-^{2}H]IGP was converted to [3-^{2}H]histidinol in triethanolamine/H_2O using the same methodology as for the reaction of unlabeled IGP in D_2O buffer. In addition to [3-^{2}H]IGP (9.9 mg, 42 μmol), the incubation mixture included HisB-containing extract (1.3 mg of protein), HisC-containing extract (26.9 mg of protein), L-glutamate (2.11 g, 12.5 mmol), and PLP (1.1 mg, 4.4 μmol). Following purification by ion exchange chromatography, the product (5.3 mg, only a portion of which was soluble in CH_3OH) was analyzed by ^{1}H and ^{2}H NMR.

1-*N*-Acetyl-4-[(2-phenyl-5-oxo-4(5*H*)-oxazolidene)methyl-^{2}*H*]-1*H*-imidazole (13). To a solution of 4(5)-[*formyl*-^{2}H]formylimidazole (**12**)[54] (487 mg, 5.02 mmol) in Ac_2O (2.83 mL) were added anhydrous NaOAc (412 mg, 5.02 mmol) and hippuric acid (899 mg, 5.02 mmol). The mixture was heated at 80 °C for 1 h and then cooled to room temperature. The resulting solid was triturated with cold H_2O (10 mL), and the remaining material was collected by vacuum filtration, washed with cold MeOH and H_2O, and dried *in vacuo*. Compound **13** was obtained as bright yellow needles (950 mg, 67%); mp 188–190 °C; ^{1}H NMR (200 MHz, DMSO-d_6) δ 2.72 (s, 3 H, CH_3), 7.14 (s, 0.08 H, CH=C), 7.58–7.77 (m, 3 H, Ph), 8.09–8.15 (m, 2 H, Ph), 8.50 (d, J = 1.2 Hz, 1 H, imidazole 4(5)H), 8.59 (d, J = 1.2 Hz, 1 H, imidazole 2H); MS (CI isobutane) *m/z* 283 (100, MH^+, $C_{15}H_{10}DN_3O_3$), 282 (13.9, MH^+, $C_{15}H_{11}N_3O_3$) X-ray data (for an analogously prepared unlabeled sample): X-ray crystallography quality crystals were obtained by dissolving **13** in a minimal amount of *p*-dioxane and adding 1–2 drops of Et_2O. Slow evaporation of the solvent through a pinhole over several days provided **13** as long, bright yellow needles. Crystal data for $C_{15}H_{11}N_3O_3$: FW = 281.27; monoclinic; a = 7.3734(5) Å, b = 24.865(2) Å, c = 18.020(2) Å, β = 98.25(1)°, V = 3269.6(9) Å^3, Z = 8, ρ_{calc} = 1.143 g/cm^3, F_{000} = 1168, m = 6.48 cm^{-1}, space group *C*2/*c* (no. 15) from systematic absences and subsequent least squares refinement.

(*Z*)-2-Benzamido-3-[imidazol-4(5)-yl][3-^{2}H]acrylic acid (14). A mixture of **13** (936 mg 3.32 mmol) and Na_2CO_3 (465 mg) in H_2O (19 mL) was heated at reflux until the azlactone had dissolved completely. The solution was then cooled in an ice bath and neutralized with acetic acid (0.30 mL). The resulting white precipitate (735 mg 86%) was collected by filtration under vacuum and dried *in vacuo* over P_2O_5: ^{1}H NMR (200 MHz, CF_3CO_2D) δ 7.47–7.92 (m, 6 H, ArH and imidazole 4(5)H), 8.72 (d, J = 1.1 Hz, 1 H, imidazole 2H).

(2*S,3*S**)-*N*-Benzoyl[3-^{2}H]histidine (15).** A mixture of **14** (700 mg, 2.71 mmol) and 10% Pd–charcoal (70 mg) in HOAc/H_2O (11:1, v/v; 42 mL) was stirred for 18 h at room temperature under 1 atm of H_2. The catalyst was removed by filtration, and the solvent was removed *in vacuo*. The residue was dissolved in 5% aqueous Na_2CO_3 (20 mL), and the resulting solution was neutralized to pH 7 with HOAc. After several hours at 0 °C, the resulting white precipitate was collected and dried *in vacuo* at 100 °C for 3 h (514 mg, 73%): mp 240–242 °C dec; ^{1}H NMR (500 MHz, CF_3CO_2D) δ 3.59 (d, J = 5.7 Hz, 1 H, C-3), 5.16 (d, J = 5.7 Hz, 1 H, C-2), 7.34–7.62 (m, 6 H, ArH and imidazole 4(5)H), 8.49 (d, J = 1.3 Hz, 1 H, imidazole 2H).

(2*S,3*S**)-[3-^{2}H]Histidinol ((2*S**,3*S**)-[3-^{2}H]5).** Reduction and deprotection of (2S*,3S*)-*N*-benzoyl[3-^{2}H]histidine (**15**) was accomplished by the method of Bauer *et al.*,[55] providing (2S*,3S*)-[3-^{2}H]histidinol–HCl: MS (CI, isobutane) *m/z* 143 (100, MH^+, $C_6H_{10}DN_3O$), 142 (10.5, $C_6H_{11}N_3O$), 125 (9.0, $C_6H_{10}DN_3O - H_2O$). A portion of this material was transformed to the free base form by ion exchange chromatography on Dowex 50W-X8 (200–400 mesh, NH_4^+), which was eluted with a stepwise pH gradient (75 mM NH_4HCO_3/NH_4OH, pH 8.0–10.5 in increments of 0.5 pH unit and a flow rate of 3.5 mL/min; 10 mL per step). Fractions (10 mL) were spotted on cellulose plates, and (2S*,3S*)-[3-^{2}H]histidinol was visualized by spraying with diazotized sulfanilic acid. The appropriate pooled fractions containing (2S*,3S*)-[3-^{2}H]histidinol were combined, and dried by lyophilization, providing the product as a fluffy white solid: ^{1}H NMR (500 MHz, CD_3OD) δ 2.73 (d, J = 6.2 Hz, 1H, C-3), 3.14 (ddd, J = 6.7, 6.2, 4.3 Hz, 1H, C-2), 3.40 (dd, J = 11.0, 6.7 Hz, 1H, C-1a), 3.57 (dd, J = 11.0, 4.3 Hz, 1H, C-2b), 6.88 (s, 1H, imidazole 4(5)H), 7.60 (s, 1H, imidazole 2H); ^{2}H NMR (76.73 MHz) δ 3.40.

Imidazoleacetol Phosphate. IAP, prepared as described previously,[12] was purified by ion exchange chromatography on a Dowex 1 cm × 8 cm (acetate form) column, which was eluting with a 0–0.5 M linear gradient of acetic acid. IAP eluted at ca. 0.15 M acetic acid, and was detected by a positive reaction with diazotized sulfanilic acid spray reagent:[56] UV–vis λ_{max} (H_2O) 215 nm (ϵ = 4474), ($MnCl_2/H_2O$) 257 nm (ϵ = 9743); ^{1}H NMR (300 MHz, 90% H_2O) (diol species) δ 3.04 (s, C-3), 3.64 (d, $J_{c,p}$ = 7.41 Hz, C-1), 7.20 (s), 8.38 (s), (keto species) δ 4.02 (s, C-3), 4.48 (d, $J_{c,p}$ = 7.32 Hz, C-1)., 7.16 (s), 8.23 (s), ^{13}C NMR (75 MHz, 90% H_2O) (diol species) δ 31.5 (C-3), 67.4 (C-1), 94.3 (C-2), 117.7, 128.1, 133.1, (keto species) δ 34.6 (C-3), 68.5 (C-1), 117.7, 126.9, 134.4, 208 (C-2); FAB HRMS (Gly) *m/z* calcd 219.0171, found 219.0184.

Spectroscopic Analysis of IAP. UV–vis Spectroscopy. IAP (0.46 mM) was incubated in 20 mM ACES (20 mM, pH 6.1), at 30 °C, in the presence of $MnCl_2$ (0.8 mM), and scanned over the range 190–500 nm every 30 s for 2 h (Figure 4).

Determination of IAP $K_d(Mn^{2+})$ via EPR Spectroscopy. IAP (1 mM) was incubated with varying concentrations of Mn^{2+} (0–2.0 mM) in HEPPS, pH 8.1, and the EPR signal of $Mn^{2+}(H_2O)_6$ was recorded. The field strength was set to 3400 G, and the microwave power and frequency were 60 mW and 9.52 GHz, respectively. The $K_d(Mn^{2+})$ of IAP and the molar ratio of Mn^{2+} bound to IAP were determined by Scatchard analysis.

Acknowledgment. We gratefully acknowledge John Kozlowski for assistance in NMR data acquisition and interpretation as well as Professor Thomas Nowak (University of Notre Dame) for his advice and assistance in the EPR studies. We thank Susan Hamilton, Tom Klem, and Dr. Carmello Bruni for histidine biosynthetic genes and enzymes. Support for this research was provided by the NIH (Grants RO1 GM36286 to J.M.S. and RO1 GM45756 to V.J.D,) and the Purdue Research Foundation (via a graduate research fellowship to A.R.P.).

Supporting Information Available: Figures showing the ^{1}H NMR spectra of IAP in 99.9% D_2O and 90%/10% H_2O/D_2O, ^{13}C NMR spectrum of IAP, and ORTEP drawing of **13** (4 pages). This material is contained in many libraries on microfiche, immediately follows this article in the microfilm version of the journal, can be ordered from the ACS, and can be downloaded from the Internet; see any current masthead page for ordering information and Internet access information.

JA951539D

(54) Battersby, A. R.; Nicoletti, M.; Staunton, J.; Vleggaar, R. *J. Chem. Soc., Perkin Trans. 1* **1980**, 43–51.

(55) Bauer, H.; Adams, E.; Tabor, H. *Biochem. Prep.* **1955**, *4*, 46–50.

(56) Rabinowitz, J. C. *Methods Enzymol.* **1963**, *6*, 703–713.